CURRENT GLOBAL REVIEWER

Half Yearly | UGC Approved | ISSN : 2319 - 8648
Issue IX Vol II , May. To Oct. 2017 | Sr. No. 64310 | Impact Factor : 2.143

Effect Of Co2+ Substitution On The Structural And Magnetic Properties Of Mg-Cu-Zn Ferrite Synthesized By Citrate Gel Combustion Method

L. M. Thorat
S. M. Dnyandeo Mohekar Mahavidyalaya Kallam Dist. Osmanabad
..... (22) ..... Dept. of Electronics .....

Abstract

The Co2+ substituted Mg-Cu-Zn ferrite nanoparticles having the molecular formula $Mg_{0.25-x}$ Co_x $Cu_{0.25}$ $Zn_{0.5}$ Fe_2O_4 (for x = 0.0, 0.05, 0.10, 0.15, 0.20) have been synthesize by citrate gel combustion method and studied by using X-ray diffraction (X R D) technique. The XRD data confirms the formation of signal phase cubic structure. The lattice constant increase with increasing Ni2+ content. We report the synthesis of nanoparticles with crystalline size is in the range of 49-51nm.The magnetic properties of the as synthesized samples were studied. The magnetic properties of the samples shows remarkable changes with change of Co2+substitutionx x.

Key Words: Ferrite, Co, Mg – Cu – Zn, X-ray diffraction. Magnetization.

1 Introduction

In recent years, the advancement in microwave technology like the wireless telecommunication systems, radar, microwave oven, medical equipment, Bluetooth technologies etc. induced a serious problem of electromagnetic pollution in this frequency range. Therefore, the demands to develop electromagnetic wave absorbers with wider absorbing bandwidths have been increased [1-8]. The electromagnetic pollution can be controlled by making use of electromagnetic absorbers and extensive studies have been carried out in this concern [9,10]. Electromagnetic wave energy can be completely absorbed and dissipated into heat through magnetic losses and dielectric losses when the impedance of free space is matched with the input characteristic impedance of an absorber [11].

Spinel ferrites have been widely utilized as electromagnetic wave absorbing materials in VHF/UHF region, due to their large magnetic losses and large resistivities [12-14]. Among the various spinel ferrites Ni-Cu-Zn ferrites have been intensively studied due to their high resistivity, low dielectric losses, high Curie temperature and excellent microwave-absorbing properties [15]. They have also been widely employed in both low and high frequency devices that play a vital role in many technological applications, such as microwave equipments, power transformers in electronics, rod antennas and read/write heads for high speed digital tape, etc [16].

The present paper is focused on the structural and magnetic properties of citrate gel synthesized $Mg_{0.25-x}Co_xCu_{0.25}Zn_{0.5}Fe_2O_4$ with X= 0, 0.05, 0.10, 0.15, 0.20 ferrites.

2 Experimental details

Synthesis of nanocrystalline $Mg_{0.25-x}Co_xCu_{0.25}Zn_{0.5}Fe_2O_4$ powders

The $Mg_{0.25-x}Ni_xCu_{0.25}Zn_{0.5}Fe_2O_4$ (x= 0, 0.05, 0.1, 0.15, 0.20) ferrites were synthesized using the citrate gel combustion method. The citrate gel combustion method is a single step, easy and economical way of synthesis of single and multicomponent oxides. This method has certain inherent advantages like low processing temperature, good stoichiometric control, homogeneous distribution of reactants and production of ultra fine particles with narrow size distribution.

The fuel citric acid is a weak acid and has three carboxylic and one hydroxyl group. These groups coordinate metal ions which enhances the homogeneous mixing of the reactants. The citric acid suppresses the precipitation of metal nitrates during water dehydration. It has electronegative oxygen atoms which interact with electropositive metal ions and therefore homogeneous single phase powders can be prepared at a relatively low temperature. Analytical reagent grade magnesium nitrate, cobalt nitrate, copper nitrate, zinc nitrate and ferric nitrate were used as starting precursors. The ratio of metal nitrates to fuel (citric acid) was kept at 3:5 moles. As per the molar composition of the

investigated systems the precursor solution was prepared and further it was heated on hot plate. Continuous heating on the hot plate converted the precursor into the gel which gets auto ignited. The auto ignition causes a rapid evolution of large volume of gases to produce voluminous powder.
The as prepared powders were collected and calcinated at 700°C for 2 h to remove traces of undecomposed fuel, nitrates (if any), and their decomposition products to obtain the pure and well crystalline powder. The calcined powder was then made into pellets using a die having 1.5 cm diameter using a hydraulic press machine and applying a pressure of 1.5 ton/cm^2 wherein polyvinyl alcohol was used as a binder. The toroids of samples were fabricated using a die having outer diameter 2 cm, inner diameter 1 cm with average height of 0.3 cm by applying a pressure of 1.5 ton/cm^2 using hydraulic press machine. All the samples in present study were sintered at 950 °C for 4 hrs in air atmosphere.

Experimental measurement

The X-ray diffraction (XRD) pattern of the samples were obtained on BRUKER D8 advanced X-ray diffractometer using Cu-Kα (λ=1.54056 Å) radiation at 2θ values between 20° to 80°. The interplanar distance d (Å) was calculated using Bragg's law. The lattice parameter of sintered samples was calculated using the formula for interplanar spacing $\frac{1}{d^2}=\frac{h^2+k^2+l^2}{a^2}$ [32] average particle size t was calculated from the Scherrer formula $t=\frac{0.9\lambda}{\beta Cos\theta}$. The X-ray density, Bulk density and Relative density were calculated by using the relation $\rho x=\frac{ZM}{Na^2}$, $\rho m=\frac{m}{\pi r^2 h}$, $\rho r=\frac{\rho m}{\rho x}\times 100$ surface morphology of the samples was studied using scanning electron microscope (Model SEM-JEOL) operating at 5 kV. Percentage porosity (P) of the samples was calculated from ρ_m and ρ_x values using the expression: $P(\%)=\left(1-\frac{\rho m}{\rho x}\right)X\ 100$
Transmission electron microscope (TEM) images were taken by using a Philips CM 200 FEG microscope equipped with a field emission gun at an accelerating voltage of 200 kV, with a resolution of 0.24nm.

3 Results and discussion

X-Ray diffraction techniquea

X-ray diffraction (XRD) was used to study the structural properties of samples in the present study. The X-ray diffraction patterns of different compositions of sintered $Mg_{0.25-x}Co_xCu_{0.25}Zn_{0.5}Fe_2O_4$ ferrites are shown in Fig. 1. The spectra revealed the presence of peaks corresponding to (3 1 1), (2 2 0), (2 2 2), (4 0 0), (4 2 2), (5 1 1), (4 4 0) and (5 3 1) planes for cubic spinel structure [17]. The peaks in the X-ray diffraction pattern were indexed using standard JCPDS File No. 08-0234.The lattice parameter (a) for various compositions is given in Table 1. No prominent effect of Co addition on the values of lattice parameter was observed. However the lattice parameter values for different samples are in close agreement with earlier reported values [18,21]. The crystallite size for different sample varies in the range of 49 nm to 51 nm and it does not shown any systematic dependency on the Co content.

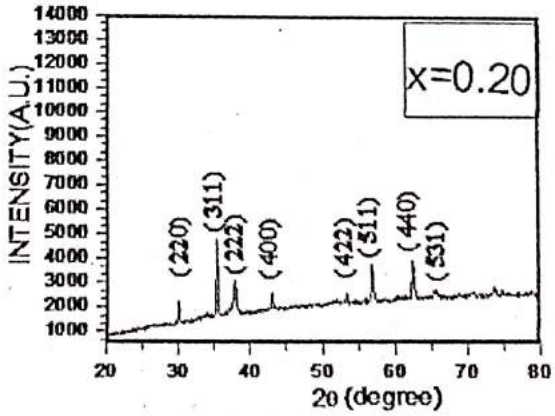

Figure 1.: X-ray diffraction patterns of the sintered $Mg_{0.25-x}Co_xCu_{0.25}Zn_{0.5}Fe_2O_4$ ferrites

The bulk density, X-ray density and relative density values for different samples in the present study are given in Table 1. Relative density increased with Co addition exhibiting maximum for x= 0.05 and 0.25. The relative density of sample with x=0.00 (Mg-Cu-Zn) is lower as compared to sample with x=0.25 (Co-Cu-Zn) which is attributed to the fact that magnesium has lower atomic weight (24.30 amu) than the cobalt (58.93 amu) atom. The replacement of Mg atoms by cobalt causes the increase in the relative density. It can also be noticed from the Table 1. that X-ray density of each sample is higher than the corresponding bulk density of sintered samples. This is attributed to the existence of the pores, which depends on sintering conditions [22].

Table 1.: Lattice parameter (a), crystallite size (D), bulk density(ρ_m), X-ray density (ρ_x) and relative density (ρ_R) of sintered $Mg_{0.25-x}Co_xCu_{0.25}Zn_{0.5}Fe_2O_4$ ferrites

X	)	t (nm)	ρ_m (gm/cm^3)	ρ_x (gm/cm^3)	ρ_R (%)
0	8.394	50	4.39	5.17	85
0.05	8.446	48	4.18	5.11	93
0.10	8.401	50	4.81	5.23	92
0.15	8.381	49	4.83	5.31	91
0.20	8.409	51	4.86	5.29	92

3.2. Magnetization – VSM studies

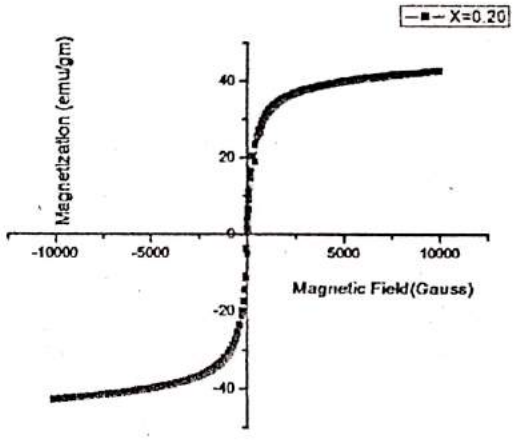

Figure 2: Magnetic hysteresis loop of sintered $Mg_{0.25-x}Co_xCu_{0.25}Zn_{0.5}Fe_2O_4$ferrites.(X=0.20)

The preferential occupancy of the cations, composition, microstructure and density of ferrites strongly influences their magnetic properties like saturation magnetization, coercivity and remenance. The room temperature hysteresis loops for various samples of sintered $Mg0.25_{-x}Co_xCu_{0.25}Zn_{0.5}Fe_2O_4$ ferrites are shown in Fig. 2. The magnetic hysteresis in case of all samples exhibited a typical shape and confirmed that the samples are magnetically ordered. The values of saturation magnetization, coercivity and remenance for all compositions are given in Table 2.

CURRENT GLOBAL REVIEWER

Half Yearly
Issue IX Vol II , May. To Oct. 2017

UGC Approved
Sr. No. 64310

ISSN : 2319 - 8648
Impact Factor : 2.143

Table2: Data on magnetic parameters like Ms, Mr./MS, n_B, Hc and relative density (ρ_R) and Curie temperature (Tc) for different compositions of sintered $Mg_{0.25-x}Co_xCu_{0.25}Zn_{0.5}Fe_2O_4$ ferrites.

X	M_s (emu)	M_r/M_s	n_B Expt.	ρ_R (%)	H_c G	D μm	T_C (°C) $\chi_{a.c.}$
0.00	239	0.0038	1.94	85	3.41	0.42	142
0.05	251	0.0056	2.03	93	5.16	1.4	153
0.10	259	0.0082	2.07	92	7.88	2.02	170
0.15	311	0.0116	2.46	91	11.04	1.58	190
0.20	288	0.0160	2.31	92	18.44	1.33	221

It is observed from the Table 2. That the increase in Co content has resulted into the increase in the value of saturation magnetization. Maximum value of saturation magnetization was exhibited by the $Mg_{0.25-x}Co_xCu_{0.25}Zn_{0.5}Fe_2O_4$ ferrite with x= 0.25. The enhancement in saturation magnetization is mainly due to the substitution of nonmagnetic Mg^{2+} ions with highly magnetic Co^{2+}. The observed variation in saturation magnetization can be explained on the basis of cation distribution and the exchange interactions between A and B-sites. It is known that the Mg ferrite is a spinel with an inversion degree of about 0.8 [23]. In Mg-Cu-Zn ferrite, the stable Zn^{2+} ions occupy the A-sites only. By substituting Co^{2+} ions for Mg^{2+} (which has a magnetic moment of 3.7 μ_B) on the octahedral sites (B-sites), an increase in the magnetization of B sublattice takes place, leading to the increase in the saturation magnetization of the ferrite [24].

Table 3: The probable cation distribution and the magnetic moment for different compositions of $Mg_{0.25-x}Co_xCu_{0.25}Zn_{0.5}Fe_2O_4$ ferrites

X	Cation distribution	n_B Th.	n_B Expt.	α_{y-k}
0.00	$(Mg_{0.025}Cu_{0.025}Zn_{0.5}Fe_{0.45})^A$ $[Mg_{0.225}Cu_{0.225}Fe_{1.55}]^BO_4$	5.999	1.94	59°16'12"
0.05	$(Mg_{0.020}Cu_{0.020}Zn_{0.5}Fe_{0.46})^A$ $[Co_{0.05}Mg_{0.180}Cu_{0.230}Fe_{1.54}]^BO_4$	6.014	2.03	58°23'56"
0.10	$(Mg_{0.015}Cu_{0.015}Zn_{0.5}Fe_{0.47})^A$ $[Co_{0.10}Mg_{0.135}Cu_{0.235}Fe_{1.53}]^BO_4$	6.048	2.07	58°8'25"
0.15	$(Mg_{0.010}Cu_{0.010}Zn_{0.5}Fe_{0.48})^A$ $[Co_{0.15}Mg_{0.090}Cu_{0.240}Fe_{1.52}]^BO_4$	6.082	2.46	54°56'42"
0.20	$(Mg_{0.005}Cu_{0.005}Zn_{0.5}Fe_{0.49})^A$ $[Co_{0.20}Mg_{0.045}Cu_{0.245}Fe_{1.51}]^BO_4$	6.121	2.31	56°13'48"

Squareness or remnant ratio (M_r/M_s) is a characteristic parameter of the material and is dependent on anisotropy. It indicates the ease with which the magnetization direction is reoriented to the nearest easy axis magnetization direction after the magnetic field is removed. The lower is its value, the more isotropic the material will be [25]. The knowledge of squareness ratio plays an essential role in the development of new materials.

The values of experimental magnetic moment and probable cation distribution are given in Table 3. The experimental magnetic moment was increased with increase in Co content however the α_{y-k} was decreased. The decrement in α_{y-k} is attributed to the replacement of nonmagnetic Mg by magnetic Co which lead to enhancement in exchange interaction.

4 Conclusions

The fine particles of $Mg_{0.25-x}Co_xCu_{0.25}Zn_{0.5}Fe_2O_4$ with X= 0, 0.05, 0.10, 0.15, 0.20, 0.25 ferrites were successfully synthesized using citrate gel combustion method. The structural properties were found to be influenced by addition of Co.. The lattice parameter of sintered samples was calculated using the formula for interplanar spacing No prominent effect of Co addition on the values of lattice parameter was observed. However the lattice parameter values for different samples are in close agreement with earlier reported values . The crystallite size for different sample varies in the range of 49 nm to 51 nm and it does not shown any systematic dependency on the Co content.

The addition of Co2+ has shown strong impact on the magnetic properties .The pulse field hysteresis loop tracer technique was used to measure the magnetic properties of Co2+substituted Mg-Cu-Zn ferrite samples.From the hysteresis loop,it is clear that the saturation magnetization and coercivity increases with increasing Co2+ substitution x.

5 References

[1] H. Bayrakdar, J. Magn. Magn. Mater. 323 (2011) 1882.
[2] V.G. Harris, IEEE Trans. Magn. 48 (2012) 1075–1104.
[3] J. L. Xie, M. Han, L. Chen, R. xiong Kuang, Long jiang Deng, J. Magn. Magn. Mater. 314 (2007) 37.
[4] M.R. Meshram, N.K. Agrawal, B. Sinha, P.S. Misra, J. Magn. Magn. Mater. 271 (2004) 207.
[5] M. Yu Ou Long jiang Deng, J. Magn. Magn. Mater. 321 (2009) 1125.
[6] K. Matsumoto, A. Kondo, T. Habu, K. Hayashi, O. Hashimoto, Microwave Opt.Technol. Lett. 48 (2006) 2065.
[7] L. Ma, G. Wang, L. Liu, B. Li, J. Alloys Comp. 505 (2010) 374.
[8] Y.N. Kazantsev, A.V. Lopatin, N.E. Kazantseva, A.D. Shatrov, V.P. Maltsev, J.Vilcakova, P. Saha, IEEE Trans. Antennas Propag. 58 (2010) 1227.
[9] J.J. Siddiqui, K. Zhu, J. Qiu, H. Ji, Mater. Res. Bull. 47 (2012) 1961.
[10] R.S. Meena, S. Bhattachrya, R. Chatterjee, Mater. Sci. Eng., B 171 (2010) 133.
[11] S.P. Gairola, V. Verma, V. Pandey, Ravi, L.P. Purohit, R.K. Kotnala, Int. J. 119 (2010) 151.
[12] Y. Nie, H. He, Z. Zhao, R. Gong, H. Yu, J. Magn. Magn. Mater. 306 (2006) 125.
[13] M. Matsumoto, Y. Miyata, IEEE Trans. Magn. 33 (1997) 4459.
[14] L. Deng, M. Han, Appl. Phys. Lett. 91 (2007) 0231191.
[15] Y . Hwang, Mater. Lett. 60(27) (2006) 3277.
[16] A Verma, D. C. Dube. J. Am. Ceram. Soc. 88(3) (2005) 519.
[17] M. P. Reddy, W. Madhuri, N. R. Reddy, K.V.S. Kumar, V.R.K. Murthy, R.R. Reddy. J Electro. Ceram. 28(1) (2012) 1.
[18] S.A. Ghodake, U.R. Ghodake, S.R. Sawant, S.S. Suryavanshi, P.P. Bakare, J. Magn. Magn. Mater. 305 (2006) 110.
[19] M. Yan, J. Hu, W. Luo, W.Y. Zhang, J. Magn. Magn. Mater. 303 (2006) 249.
[20] H. Su, H. Zhang, X. Tang, B. Liu, Z. Zhong, Journal of Alloys and Compounds 475 (2009) 683.
[21] A. Daigle, J. Modest, A.L. Geiler, S. Gillette, Y. Chen, M. Geiler, B. Hu, S. Kim, K. Stopher, C. Vittoria, V.G. Harris, Nanotechnology 22 (2011) 305708.
[22] M. P. Reddy, I.G. Kim, D. S. Yoo, W. Madhuri, M. V. Ramana, A. Shaaban, N. R. Reddy, K.V. S. Kumar, R. R.Reddy, Superlatt. Micros. 56 (2013) 99.
[23] J. Smit, H.P.J. Wijn, Les Ferrites, Dunod, Paris, 1961.
[24] H. Su, H. Zhang, X. Tang, J. Magn. Magn. Mater. 302 (2006) 278.
[25] A.R. Bueno, I.M. Gregori, M.C.S. Nobrega, Mater. Chem. Phys. 105 (2007) 229.